AIAA Infotech@Aerospace 2010
20 - 22 April 2010, Atlanta, Georgia

AIAA 2010-3416

Adaptive Control of Quadrotor UAVs in the Presence of Actuator Uncertainties

Zachary T. Dydek[1], Anuradha M. Annaswamy[2]
Massachusetts Institute of Technology, Cambridge, MA, 02139

and

Eugene Lavretsky[3]
The Boeing Company, Huntington Beach, CA, 92647

This paper describes the application of model reference adaptive control on a light-weight, low-cost quadrotor UAV platform. An adaptive controller was designed to augment an existing linear controller that provides autonomy and waypoint following. The design of the adaptive controller is driven by Lyapunov stability arguments and has a proof of stability grounded in a nonlinear framework. The approach was validated using flight testing inside an indoor test facility. The adaptive controller was found to offer increased robustness to parametric uncertainties. In particular, it was found to be effective in mitigating the effects of a loss of thrust anomaly, which may occur due to component failure or physical damage. The design of the adaptive controller is presented, followed by a comparison of flight test results using the existing linear and augmented adaptive controllers.

Nomenclature

x	Position in x-direction
y	Position in y-direction
z	Altitude
ϕ	Roll angle
θ	Pitch angle
ψ	Yaw angle
U_1	Collective control force
U_2	Roll control force
U_3	Pitch control force
U_4	Yaw control force
g	Acceleration due to gravity
m	Mass
I_x	Moment of Inertia about the x-axis
I_y	Moment of Inertia about the y-axis
I_z	Moment of Inertia about the z-axis
J_R	Moment of Inertia of the rotor blades
Ω_R	Angular velocity of the rotor blades
x_p	State vector for the linearized dynamics
Λ	Actuator uncertainty
u	Control input vector
r	Reference command

[1]PhD Candidate, Department of Mechanical Engineering, Room 3-441, AIAA Student Member.
[2]Senior Research Scientist, Department of Mechanical Engineering, Room 3-339A, AIAA Member.
[3]Senior Technical Fellow, 5301 Bolsa Avenue, Mail Code H013-B318, AIAA Associate Fellow.

y_p System output
e_y Output tracking error
x_t Extended state vector
y_t Extended system output
u_{nom} Nominal control input
u_{ad} Adaptive control input
$\hat{\theta}$ Adaptive parameters
ω Linear regressor vector
Γ Adaptive gains
e Model reference error
dz Dead-zone width
$\theta^{\max}$ Bound on adaptive parameters

I. Introduction

Quadrotor helicopters have been an increasingly popular research platform in recent years. Their simple design and relatively low cost make them attractive candidates for swarm operations, a field of ongoing research in the UAV community. In designing a controller for these aircraft, there are several important considerations. There are numerous sources of uncertainties in the system–actuator degradation, external disturbances, and potentially uncertain time delays in processing or communication. These problems are only amplified in the case of actuator failures, where the aircraft has lost some of its control effectiveness. Additionally, the dynamics of quadrotors are nonlinear and multivariate. There are several effects to which a potential controller must be robust: the aerodynamics of rotor blade (propeller and blade flapping), inertial anti-torques (asymmetric angular speed of propellers), as well as gyroscopic effects (change in orientation of the quadrotor and the plane of the propeller). References [1–4] further detail the challenges in designing a controller for UAVs with nonlinear dynamics and parameter uncertainties.

The redundancy in the actuators of a quadrotor makes them robust towards a set of partial failures. Though the performance and maneuverability will most likely be reduced in the case of such a failure, it is desirable for a controller to stabilize the system and allow for reduced mode operations such as a safe return, stable hover, etc. Adaptive control is an attractive candidate for this aircraft because of its ability to generate high performance tracking in the presence of parametric uncertainties.

This paper is organized as follows. Section 2 describes the experimental setup and existing control architecture. Section 3 describes the development of the adaptive controller. Flight test results are shown in Section 4 and conclusions and future directions are discussed in Section 5. An appendix detailing some of the finer points of the implementation, including robustness modifications to deal with noisy signals and selection of the adaptation rates follows.

II. Experimental Setup

The Aerospace Controls Laboratory at MIT utilizes a UAV testbed facility known as RAVEN (Real-time indoor Autonomous Vehicle test ENvironment). RAVEN uses a Vicon motion capture system to enable rapid prototyping of aerobatic flight controllers for helicopters and aircraft; robust coordination algorithms for multiple helicopters; and vision-based sensing algorithms for indoor flight[5,6]. The Aerospace Controls Laboratory also operates several Draganflyer quadrotors autonomously using a simple, ground-based controller. The RAVEN system essentially consists of a vision based motion capture system that provides 6DoF pose parameters at fixed frequency of 100Hz. Commands are sent to the quadrotors using a USB wireless remote-control module. The system operates on a cluster of Linux workstations, with each node assigned to the control of an individual UAV. This system is used to run the vehicle flight controller and other path planning algorithms. The adaptive controller is then implemented and run alongside the fixed-gain controller. This system allows for flight testing of the quadrotor using both baseline (fixed-gain) and adaptive controllers.

With the capabilities and limitations of RAVEN in mind, a flight control system is designed for the quadrotor which primarily addresses the problem of actuator uncertainty. An augmented adaptive control approach is utilized

Figure 1. Draganflyer four rotor helicopter UAVs in the Real-time indoor Autonomous Vehicle test ENvironment (RAVEN).

with the existing fixed-gain controller as a baseline. This adaptive controller is based on nonlinear stability theory, the details of which have been touched on by many authors throughout the years[7–11]. The augmented structure of the adaptive controller implies that in the nominal case, that is the case with no parameter uncertainty, the overall system is equivalent to the baseline control. However, when failures or other uncertainties arise, the adaptive controller works to assist the baseline controller in maintaining stability and performance.

III. Development of the Adaptive Controller

The dynamics of quadrotor helicopters have been studied in detail by several groups[12,13]. A simple, rigid-body model of the quadrotor which assumes low speeds is given by:

$$\begin{aligned}
\ddot{x} &= (\cos\phi\sin\theta\cos\psi + \sin\phi\sin\psi)\frac{U_1}{m} \\
\ddot{y} &= (\cos\phi\sin\theta\sin\psi - \sin\phi\cos\psi)\frac{U_1}{m} \\
\ddot{z} &= -g + (\cos\phi\cos\theta)\frac{U_1}{m} \\
\\
\ddot{\phi} &= \dot{\theta}\dot{\psi}\left(\frac{I_y - I_z}{I_x}\right) - \frac{J_R}{I_x}\dot{\theta}\Omega_R + \frac{L}{I_x}U_2 \\
\ddot{\theta} &= \dot{\phi}\dot{\psi}\left(\frac{I_z - I_x}{I_y}\right) + \frac{J_R}{I_y}\dot{\phi}\Omega_R + \frac{L}{I_y}U_3 \\
\ddot{\psi} &= \dot{\phi}\dot{\theta}\left(\frac{I_x - I_y}{I_z}\right) + \frac{1}{I_z}U_4
\end{aligned} \tag{1}$$

where x, y, and z are the position of the center of mass in the inertial frame; ϕ, θ, and ψ are the Euler angles which describe the orientation of the body-fixed frame with respect to the inertial frame; m, I_x, I_y, and I_z are the mass and moments of inertia of the quadrotor respectively; and J_R and Ω_R are the moment of inertia and angular velocity of the propeller blades. U_1, U_2, U_3, and U_4 are the collective, roll, pitch, and yaw forces generated by the four propellers. For the purposes of control design, we can linearize the dynamics in (1) about the hover position. This linear system

is used for the design of the adaptive controller as detailed below.

A. Problem Statement

We can write the linearized dynamics as

$$\dot{x}_p = A_p x_p + B_p \Lambda u, \tag{2}$$

where $B_p \in \Re^{nxm}$ is constant and *known*, $A_p \in \Re^{nxn}$ is constant and *unknown*, $x_p \in \Re_p^n$, $u \in \Re^m$, $\Lambda \in \Re^{mxm}$ is an unknown diagonal positive definite constant matrix with diagonal elements $\Re \in (0, 1]$. The goal is to track a reference command $r(t)$ in the presence of the unknown A_p, and Λ. We define the system output as

$$y_p = C_p x_p. \tag{3}$$

In the case of the quadrotor, the output states are the x, y, z, and ψ. The output tracking error is then given by

$$e_y = y_p - r, \tag{4}$$

Augmenting (2) with the integrated output tracking error

$$\dot{e}_{y_I} = e_y, \tag{5}$$

leads to the extended open loop dynamics

$$\dot{x_t} = A_t x_t + B_t \Lambda u + B_c r. \tag{6}$$

where $x_t = \begin{bmatrix} x_p^T & e_{y_I}^T \end{bmatrix}^T$ is the extended system state vector. The extended open-loop system matrices are given by

$$A_t = \begin{bmatrix} A_p & 0 \\ C_p & 0 \end{bmatrix},\ B_t = \begin{bmatrix} B_p \\ 0 \end{bmatrix},\ B_c = \begin{bmatrix} 0 \\ -I \end{bmatrix}, \tag{7}$$

and the extended system output

$$y_t = \begin{bmatrix} C_p & 0 \end{bmatrix} x_t = C_t x_t. \tag{8}$$

B. Reference Model

A nominal controller

$$u_{nom} = K_x x_t, \tag{9}$$

can be designed for the system in (6) in the case where there is no uncertainty, that is $\Lambda = I^{nxn}$. The feedback gains K_x can be selected using LQR or classical design techniques. The reference model used by MRAC is the closed loop system given by (6), again in the case of no uncertainty, along with the control input in (9)

$$\dot{x}_m = A_t x_m + B_t u_{nom} + B_c r = A_m x_m + B_c r. \tag{10}$$

C. Adaptive Controller

An adaptive control input is added to the baseline controller as

$$u_{ad} = \hat{K}_x^T x_t + \hat{\theta}_r^T r + \hat{\theta}_d = \hat{\theta}^T \omega, \tag{11}$$

where $\hat{\theta}^T = \begin{bmatrix} \hat{K}_x^T & \hat{\theta}_r^T & \hat{\theta}_d^T \end{bmatrix}$ are time-varying adaptive parameters that will be adjusted in the adaptive law given in (13) below and $\omega^T = \begin{bmatrix} x_t^T & r^T & 1 \end{bmatrix}$ is the regressor vector. The overall control input is thus

$$u = u_{ad} + u_{nom} = \hat{\theta}^T \omega + K_x x_t + r. \tag{12}$$

The canonical adaptive law is given by

$$\dot{\hat{\theta}} = -\Gamma \omega e^T P B_t, \tag{13}$$

where Γ is a diagonal positive definite matrix of adaptive gains, $e = x - x_m$ is the model tracking error, and P is the unique symmetric positive definite solution of the Lyapunov equation,

$$A_m^T P + P A_m = -Q, \tag{14}$$

where Q is also symmetric positive definite. The stability of this system is a well known result in adaptive control[7,14].

IV. Flight Test Results

In the following series of tests, the quadrotor UAVs are commanded to hover in a fixed position. A simulated loss of control effectiveness is then injected into the system and the resulting performance is compared using both the baseline (fixed-gain) controller and the augmented adaptive controller.

Figure 2 shows a birds-eye view of the trajectory traced by each controller and the deviation from the commanded hover position, here marked as (0,0). As the rotor in the positive x-direction loses 45% of its thrust, the resulting moment about the y-axis causes the quadrotor to increase its pitch angle. This has the effect of vectoring the collective thrust, causing the UAV to accelerate in the positive x-direction. This failure also results in a loss of altitude as well as a yaw moment. All four rotors must work quickly and effectively to overcome the sudden change in the dynamics due to the loss of thrust. Because the nominal controller contains integrators on the x and y axes, it eventually does return to the commanded position. The adaptive controller is faster to react to the change in dynamics and returns to within 15 cm of the commanded position in 20% less time than the nominal controller. The maximal radius of departure for the adaptive controller is 46% less than that of the nominal controller. This can be a critical difference in the case of formation flying, swarm operations, or when operating in a cluttered environment.

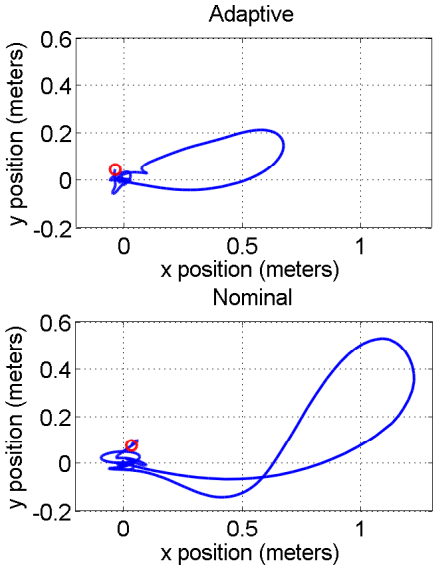

Figure 2. Birds-eye view of the quadrotor trajectory following a 45% loss of thrust in one actuator. The initial position of the quadrotor is with the failed actuator pointing in the positive x direction. The red circles denote the quadrotor position at the end of the test period.

In figure 3, the same flight test is performed with a more severe, 50% loss of thrust failure. In this example, the nominal controller was not sufficient to prevent a crash. The UAV was accelerating toward the wall of the indoor testbed when the kill switch was thrown. If the quadrotor had sufficient time and space, it is possible that it may have recovered from this particular failure. However, a departure radius of over 3 meters is unacceptable for many applications.

Figure 4 shows the pitch angle for the maneuver shown in figure 2. The adaptive controller quickly corrects for the change in dynamics before the pitch angle becomes excessive, thus staying closer to the linear operating condition for which the baseline controller is designed.

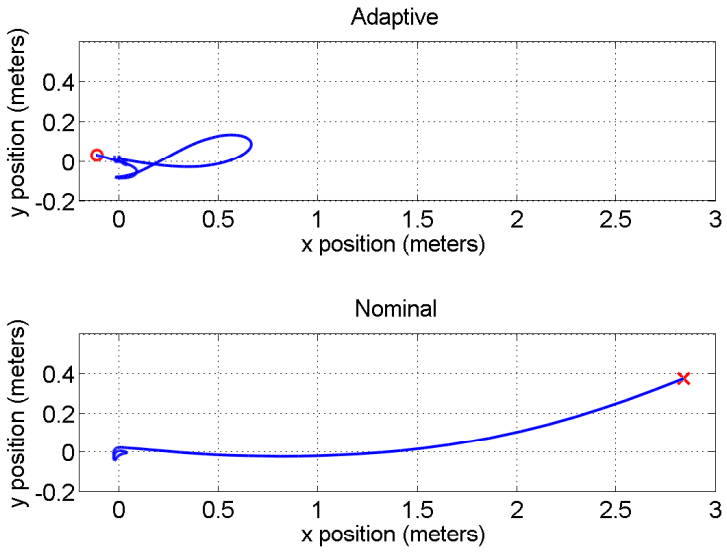

Figure 3. Birds-eye view of the quadrotor trajectory following a 50% loss of thrust in one actuator. The initial position of the quadrotor is again with the failed actuator pointing in the positive x direction. In the adaptive control case, the red circle denotes the quadrotor position at the end of the test period. In the nominal control case, the red X denotes the quadrotor position at the time when the controller kill switch was flipped. At this moment in time, the quadrotor was accelerating towards one of the walls of the testbed.

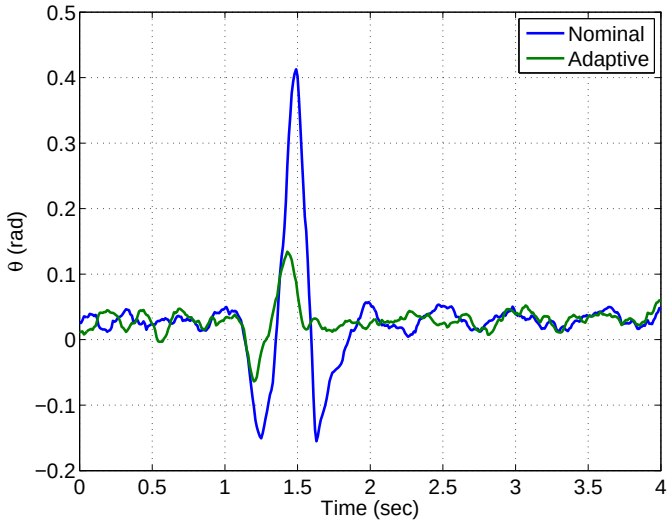

Figure 4. Pitch angle comparison of nominal and adaptive controllers in the 45% loss of thrust failure case. The time scale is shifted so that the failure occurs at $t = 1$. The adaptive controller exhibits significantly less deviation from level flight.

However, the improved performance comes at a cost of increased control effort. In particular, if we examine the FFT of the control signals for both the baseline and adaptive controllers during the first second after the failure occurs, we can see that the adaptive controller is using significantly more control power. Figure 5 shows this comparison. In

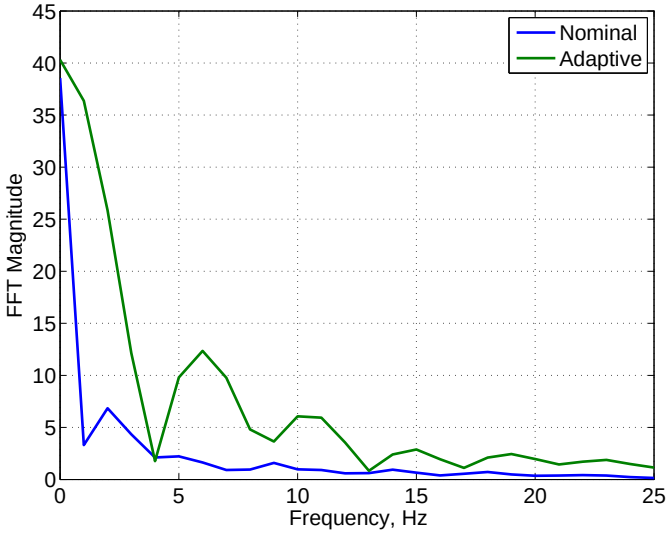

Figure 5. FFT of control signals of the baseline and adaptive controllers during the 1 second interval after failure occurs.

our application, this level of control usage is acceptable. However, under a different set of constraints, this level of controller operation may be excessive. Some of our future work involves developing control algorithms which give improved performance with minimal additional control effort.

V. Conclusion

A description of an adaptive controller based on Lyapunov stability and its application to a quadrotor UAV was presented. Flight testing was carried out in an indoor test facility using both baseline and model reference adaptive controllers. It was shown that the adaptive controller offers several benefits over the existing fixed-gain approach,

particularly in the case of actuator failures. For less severe failures, the adaptive controller was faster in reacting to changes in dynamics, resulting in a decreased radius of departure. For more severe failures, the adaptive controller prevented a crash and allowed for safe operation and landing. It was found that the adaptive controller used more control effort during the period directly following the insertion of the failure. For this particular application, the added robustness to parameter uncertainty outweighs the increased control effort.

Appendix

This appendix details some of the implementation issues which were not covered in the main text. The adaptive controller described in Section III..C. was implemented in C++ to run alongside the existing linear controller. Due to sensor noise in the system, it was found that a dead-zone modification was required to avoid parameter drift. Instead of adapting to the error e, we adapt to the modified error e_{dz}, which is given by

$$e_{dz} = \begin{cases} e + dz & \text{if} \quad e < -dz \\ 0 & \text{if} \quad -dz < e < dz \\ e - dz & \text{if} \quad e > dz. \end{cases} \tag{15}$$

The size of the dead-zones dz was selected to be just larger than the sensor noise, which mitigated parameter drift without having significant effect on the performance of the adaptive controller. The adaptive law given in (13) was also modified to include the projection operator, which provides bounds on the adaptive parameters. The projection operator is defined column-wise for the j^{th} column as

$$\text{Proj}(\theta_j, y_j) = \begin{cases} y_j - \frac{\nabla f(\theta_j)(\nabla f(\theta_j))^T}{||\nabla f(\theta_j)||^2} y_j f(\theta_j), & \text{if} \quad f(\theta_j) > 0 \quad \text{and} \quad y_j^T \nabla f(\theta_j) > 0, \\ y_j, & \text{otherwise} \end{cases} \tag{16}$$

where the convex function f is given as

$$f(\theta_j) = \frac{||\theta_j||^2 - \left(\theta_j^{\max}\right)^2}{\epsilon_j \left(\theta_j^{\max}\right)^2} \tag{17}$$

The new adaptive law is given column-wise by

$$\dot{\hat{\theta}}_j = -\Gamma \text{Proj}(\hat{\theta}_j, (\omega e_{dz}^T P B)_j), \tag{18}$$

This ensures that the adaptive parameters $\hat{\theta}$ are less than some prescribed bound $\theta^{\max}$. Along with the dead-zone modification, this changes the stability result for the adaptive controller from a global to a semi-global result.

It was also found that frame misalignment could result in non-zero error terms even in the no-failure case. This results in the dead-zones mentioned above to be slightly off-center, which can cause parameters to drift. A 10 sec period of hover is sufficient to determine the actual hover attitude, which is then used to adjust the error terms so that they are centered at 0. This is equivalent to slightly adjusting the point about which the system is linearized, and does not have any effect on the stability result.

Another important implementation issue is the selection of the adaptive gains. According to the theory described in Section III..C., any choice of adaptive gains results in the same stability result. In practice, however, it was found that nonlinearities, unmodeled dynamics, actuator saturation, and particularly time delay caused instabilities at higher adaptive gains such as the one shown in figure 6. Figure 6(a) shows the response of the roll rate and roll command with a 45% loss of actuator effectiveness in one motor. Figure 6(b) shows the same response, only with adaptive gains increased by 25%. Through some combination of actuator saturation and time delay, the signals become completely out-of-phase and the system becomes unstable, causing an eventual crash.

To select the adaptive gains, we employed the following empirical formula, which arises from inspection of the structure of the adaptive laws[15]

$$\Gamma = \left| \frac{\text{diag}(\vartheta)}{\tau_{min} p r_{max}} \right| + \Gamma_0 \tag{19}$$

where

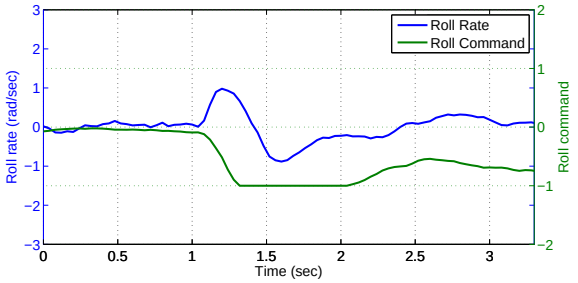

(a)

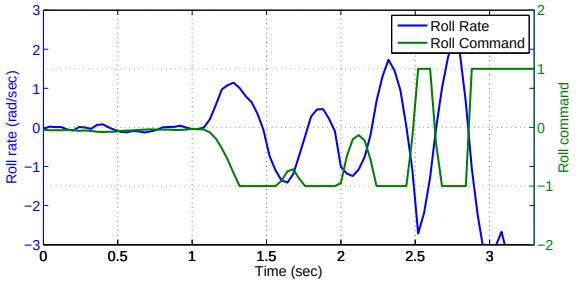

(b)

Figure 6. Response to a 45% loss of actuator effectiveness for the adaptive controller with (a) nominal adaptive gains, (b) adaptive gains increased 25% over nominal.

i. $\vartheta \in \Re^n$ is vector given by the sum of the columns of $\bar{\theta}^*$ where $\bar{\theta}^*$ corresponds to the uncertainty $\Lambda = \bar{\Lambda}$ for which the plant has the most unstable eigenvalues. The components of $\bar{\theta}^*$ are given by

$$\begin{aligned} \bar{K}_x^* &= -K_x \bar{\Lambda}^{-1}, \\ \bar{\theta}_r^* &= \bar{\Lambda}^{-1}, \\ \bar{\theta}_d^* &= 1_{1\text{x}m}. \end{aligned} \tag{20}$$

ii. τ_{min} is the smallest time constant of the reference model,

iii. p is the norm of $B^T P$,

iv. r_{max} is the maximum amplitude of the reference input signal,

v. Γ_0 is a small positive definite diagonal matrix which ensures that Γ is positive definite.

The resulting adaptive gains were then manually tuned to achieve desired response in each axis.

Acknowledgments

This research is funded by the Boeing Company Strategic University Initiative. We would like to acknowledge Prof. Jonathan How, Buddy Michini, and Josh Redding at the Aerospace Controls Laboratory at MIT for their help and allowing the use of the RAVEN testbed.

References

[1]Benallegue, A., Mokhtari, A., and Fridman, L., "High-order sliding-mode observer for a quadrotor UAV," *International Journal of Robust and Nonlinear Control*, Vol. 18, No. 4, 2008, pp. 427–440.

[2]Kim, J., *Model-Error Control Synthesis: A new Approach to Robust Control*, Ph.D. thesis, Texas A&M University, 2002.

[3]Castillo, P., Lozano, R., and Dzul, A., *Modelling and control of mini-flying machines*, Springer-Verlag New York Inc, 2005.

[4]Schwager, M., Annaswamy, A. M., and Lavretsky, E., "Adaptation-Based Reconfiguration in the Presence of Actuator Failures and Saturation," *Proc. American Control Conference*, Portland, Oregon, June 2005, pp. 2640–2645.

[5]Tournier, G., Valenti, M., How, J., and Feron, E., "Estimation and control of a quadrotor vehicle using monocular vision and moirè patterns," *AIAA Guidance, Navigation and Control Conference and Exhibit*, Citeseer, 2006, pp. 21–24.

[6]Valenti, M., Bethke, B., Fiore, G., How, J., and Feron, E., "Indoor multi-vehicle flight testbed for fault detection, isolation, and recovery," *Proceedings of the AIAA Guidance, Navigation, and Control Conference and Exhibit, Keystone, CO*, 2006.

[7]Narendra, K. S. and Annaswamy, A. M., *Stable Adaptive Systems*, Prentice-Hall, Englewood Cliffs, NJ, 1989.

[8]Ioannou, P. A. and Sun, J., *Robust Adaptive Control*, Prentice-Hall, Upper Saddle River, NJ, 1996.

[9]Sastry, S. and Bodson, M., *Adaptive control: stability, convergence, and robustness*, Prentice-Hall, Englewood Cliffs, NJ, 1989.

[10]Slotine, J. J. E. and Coetsee, J. A., "Adaptive sliding controller synthesis for nonlinear systems," *International Journal of Control*, Vol. 43, No. 6, 1986, pp. 1631–1651.

[11]Krstic, M., Kokotovic, P., and Kanellakopoulos, I., *Nonlinear and adaptive control design*, John Wiley & Sons, New York, NY, USA, 1995.

[12]Bouabdallah, S., Murrieri, P., and Siegwart, R., "Design and control of an indoor micro quadrotor," *IEEE International Conference on Robotics and Automation*, Vol. 5, Citeseer, 2004, pp. 4393–4398.

[13]Hoffmann, G., Huang, H., Waslander, S., and Tomlin, C., "Quadrotor helicopter flight dynamics and control: Theory and experiment," *Proc. of the AIAA Guidance, Navigation, and Control Conference*, Citeseer, 2007.

[14]Kreisselmeier, G. and Narendra, K. S., "Stable Model Reference Adaptive Control in the Presence of Bounded Disturbances," *IEEE Transactions on Automatic Control*, Vol. 27, No. 6, December 1982, pp. 1169–1175.

[15]Dydek, Z. T., Jain, H., Jang, J., Annaswamy, A. M., and Lavretsky, E., "Theoretically Verifiable Stability Margins for an Adaptive Controller," *Proc. AIAA Conference on Guidance, Navigation, and Control*, Keystone, Colorado, August 2006, AIAA-2006-6416.